Standing acoustic waves imaged by a nanomechanical resonator

F. W. Beil, R. H. Blick, Achim Wixforth

Angaben zur Veröffentlichung / Publication details:

Beil, F. W., R. H. Blick, and Achim Wixforth. 2004. "Standing acoustic waves imaged by a nanomechanical resonator." *Physica E: Low-dimensional Systems and Nanostructures* 21 (2-4): 1106–10. https://doi.org/10.1016/j.physe.2003.11.188.

Standing acoustic waves imaged by a nanomechanical resonator

F.W. Beil[a,*], R.H. Blick[b], A. Wixforth[c]

[a] *Center for NanoScience, LMU München, Geschwister-Scholl-Platz 1, München D-80539, Germany*
[b] *Electr. and Comp. Engineering, University of Wisconsin-Madison, 1415 Engineering Drive, Madison WI 53706, USA*
[c] *Lehrstuhl für Experimentalphysik I, Universität Augsburg, Universitätsstrasse 1, Augsburg D-86125, Germany*

Abstract

A nanomechanical beam resonator is used to image the standing wave pattern formed by two counter propagating surface acoustic waves of the Rayleigh type. As the intrinsic properties of the resonator are affected by a fast off-resonant mechanical excitation, it is possible to scan the wave pattern when shifting the positions of the wave's knots through the resonator's position. Due to the small size of the beam the wave is hardly disturbed by the nanoresonator, and the observed shifts in the resonator's eigenfrequency follow the expected form of a standing wave. At high acoustic amplitudes deviation from the linear behavior is observed while the dependence of the effect on the beam's magneto-impedance probe power elucidates the physical origin of the resonator tuning.

Keywords: Nanomechanics; Surface acoustic waves

Nanomechanical resonators are sensitive tools to measure ultra-small forces and charges when operated in resonance. Due to their size these mechanical systems exhibit eigenfrequencies up to 1 GHz, with quality factors of 10 000 and more [1]. A convenient technique to probe the dynamical properties of these resonators is traditional magneto-impedance spectroscopy [2], as used in some sensor applications. There, a shift of the resonance frequency of the sensors is used to detect the measurand. As the intrinsic properties of a nanobeam are effectively tuned by fast off-resonant mechanical excitation [3,4], it is possible to detect acoustic waves interacting with a nanomechanical resonator by the induced shift of its eigenfrequency.

Surface acoustic waves (SAW) are perfectly suited to interact with nanobeams as their typical frequencies and amplitudes have the order of magnitude characteristic for nanomechanical beam resonators. They are easily generated at a well-defined frequency by interdigitated structures called interdigital transducers (IDTs) (comp. Fig. 1(b)). A voltage applied to the collection electrodes drops between each finger pair and due to the inverse piezo-effect stresses the material underneath. If an AC signal at the resonance frequency $f_{saw} = v_{saw}/\lambda$ is applied, a coherent acoustic beam, propagating along the samples surface, is generated. Here f_{saw} denotes the frequency, v_{saw} the velocity and λ the wavelength of the SAW. The wavelength of the SAW is determined by the

* Corresponding author. Fax: +0049-089-2180-3182.
E-mail address: florian.beil@physik.uni-muenchen.de (F.W. Beil).

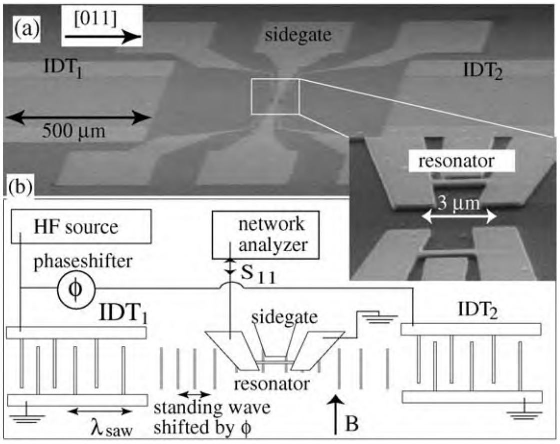

Fig. 1. (a) Micrograph of the delayline with freely suspended beam resonators placed in the line of fire of two opposite IDTs forming a delayline. (b) Experimental setup to measure the interaction of the beam with a standing acoustic wave. The dynamic properties of the beam are probed by magneto-impedance spectroscopy, while the standing wave can be shifted along the sample by scanning the phase difference between IDT_1 and IDT_2.

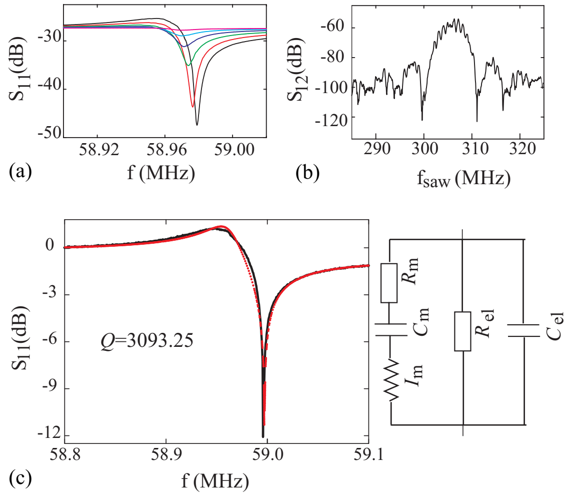

Fig. 2. (a) Magneto-impedance spectrum of the resonator's eigenmode at a driving power of Pres $= -50$ dBm and temperature of 4.2 K. With decreasing magnetic field the signal disappears, proofing its mechanical origin. (b) The spectrum of the SAW shows maximum generation of acoustic power at 303 MHz. (c) The equivalent circuit model of the beam probed by magneto-impedance spectroscopy. The curve calculated from this model follows the non-Lorentzian features of the measured resonance and yields a quality factor $Q = 3093$.

lithographically defined IDT finger spacing whereas the penetration depth of the SAW is of the same order as the wavelength. Two identical IDTs in series form a 'delayline', which can also be used to generate standing waves by launching counter propagating phase-locked SAW with identical frequency. In the sound path of these IDTs we place a nanomechanical beam resonator. The freely suspended beams are produced by standard techniques described in detail earlier [5]. In Fig. 1(a) a micrograph of the samples setup together with a close-up of the beam are shown. For the measurements presented here the beam had a length $L \sim 3$ µm, height of 200 nm and width of 300 nm. The SAW wavelength λ_{saw} was matched to approximately twice the length of the beam $\lambda_{saw} = 2L$ (taking into account additional underetching of the beam's clamping points). Then the acoustic strain induced in the beam by the SAW becomes largest [4]. To excite and detect the resonator's motion we apply magneto-impedance spectroscopy [2]. This method detects motion-induced changes of the beam's impedance via the reflected RF signal at the resonator. The resonant motion is driven by the Lorentzian forces acting on the beam, when placed in a strong DC magnetic field and applying an AC signal at the beam's resonance frequency f_0 to the conducting layer. Typical traces for a resonator operating at 59.97 MHz are depicted in Fig. 2(a). Decreasing the magnetic field decreases the detected signal, which is an evidence for the mechanical origin of the resonance. To detect the influence of additional acoustic excitation on the beam's resonance we apply a driving signal with frequency f_{saw} to the IDTs and trace the changes in the reflected signal at the beam. The SAW passes under the freely suspended beam, coupling to its clamping points. The anchoring points of the beam have to follow the elliptic particle motion induced by the plane-polarized Rayleigh wave. As f_{saw} is considerably higher than f_0 direct cross talk of the IDTs to the beam as well as cross talk of the SAW's piezoelectric fields to the conducting layer play no role when detecting at the beam's eigenfrequency. When applying two phase-locked signals of the same frequency within the IDT's bandpass to the two IDTs, a standing acoustic wave over the delayline is formed. By changing the relative phase between the two IDTs the standing wave pattern can be moved over the beam's region. Again the reflected signal at the beam is measured against the relative phase between the two IDTs. To characterize the SAW we measured the transmission of acoustic power over the delayline from IDT_1 to IDT_2 (comp. Fig. 1(b)). In Fig. 2(b) the measured bandpass of the acoustic delayline with a center frequency f_{saw} of 303 MHz is shown. The beam's resonance in Fig. 2(a), observed as a dip in the reflected signal, shows deviations from the expected Lorentzian shape. Due to the small beam under investigation we have to take into account the electric environment in which it is embedded, and model the whole setup (comp. Fig. 2(c)). The mechanical resonator is incorporated into this model by choosing an appropriate equivalent circuit [6], which results in the same equation of motion as the mechanical model. For this reason, we model the beam by a series circuit of a mechanical resistance R_{m}, capacitance C_{m}, and inductance I_{m}. Here R_{m} models the inherent anelastic losses in the beam. Parallel to that an electrical resistance R_{e} and capacitance C_{e} are introduced to model the losses and capacitances of the setup's wiring. The impedance of this model Z is calculated and the measured traces are fitted to the coefficient of reflection S_{11}:

$$S_{11} = \left| \frac{Z - 50\ \Omega}{Z + 50\ \Omega} \right|. \tag{1}$$

In Fig. 2(c) we compare a fit obtained by the method described above to the measured resonance. The calculated curve closely follows the measured trace and nicely exhibits its non-Lorentzian features. When applying an acoustic load, the dynamic properties of the beam are modified [3]. A SAW of the Rayleigh-type propagating in the [0 1 1] direction on GaAs is plane polarized in the sagittal plane, which is defined via the x-axis in [0 1 1] direction (cf. Fig. 1), and the y-axis perpendicular to x and the samples surface. If two counter propagating SAW with relative phase shift ϕ form a standing wave the beam's clamping points have to follow an elliptic particle motion in the sagittal plane, specified by A_{t} and A_{l}, the transversal resp. longitudinal components of the SAW. The amplitude at a certain point x depends on the relative phase between driving signals at IDT_1 and IDT_2. The typical

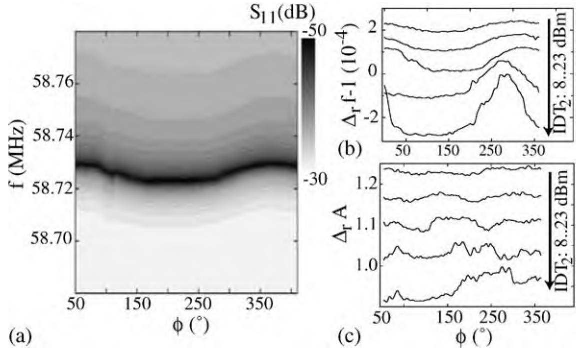

Fig. 3. (a) Shift of the resonance shown in Fig. 2(a) by a standing acoustic wave. The phase between IDT_1 and IDT_2 was scanned resulting in a lateral shift of the standing wave by half a wavelength. (b) When increasing the amplitude of the standing wave we observe a non-linear deviation from the sine dependence on ϕ for large SAW amplitudes. The power applied at IDT_1 was 2 dBm. (c) The dependence of the resonators amplitude on ϕ shows features similar to the shift in eigenfrequency in (b).

SAW amplitudes are a few Å, whereas the typical amplitudes of the beam's motion are in the same range. The fast excitation of the beam's clamping points induces stresses in the resonator which shift the eigenfrequency and internal damping of the beam [3,4]. This dependence on acoustic loading can be used to map the pattern of a standing acoustic wave. In Fig. 3(a) we plot the modulation of the beam's resonance while scanning the relative phase ϕ of the driving signals applied to the two IDTs of the delayline. The trace resembles the form of a standing wave, which laterally is swept through the beam's position. By keeping the driving power at IDT_1 constant at 2 dBm and increasing the phase locked signal at IDT_2 from 3 up to 23 dBm we sweep the acoustic power in the standing wave. As the acoustic coupling of IDT_1 was considerably better than that of IDT_2 a balance of right and left travelling SAW is achieved when applying higher driving powers at IDT_2. In Fig. 3(b) we plot the relative shift Δf_{r} of the resonator's eigenfrequency and amplitude on phase for different driving powers at IDT_2. Here

$$\Delta f_{\mathrm{r}} = \frac{f_{\phi}}{f_{\mathrm{unloaded}}}, \tag{2}$$

where f_ϕ is the measured eigenfrequency at relative IDT phase ϕ, and f_{unloaded} is the acoustically unloaded eigenfrequency. At low amplitudes of the standing wave the shift of the beam eigenfrequency shows a sine like behavior, the expected image of the standing acoustic wave. When increasing the amplitude of the SAW we observe the maximum frequency shift to be localized around $\phi = 300$, whereas the curve is no longer sinusoidal. The resonator amplitude in Fig. 3(b) exhibits a reduced amplitude for the same phase shifts ϕ at which the eigenfrequency of the resonator is modified by the standing SAW. The traces obtained by this method reflect the degree of mechanical excitation for the resonator's position in a standing acoustic wave. Whenever the relative phase between IDT_1 and IDT_2 is adjusted such that a SAW node coincides with the beam center, a maximum effect is expected. In that case, the SAW-driven motion of the suspensions acts in opposite directions, and the SAW exerts maximum forces on the beam. Vice versa, a small effect on the resonator is expected whenever the beam center is located at a maximum of the standing wave. Here, the two clamping points move in phase and the only force acting on the nanoresonator is a rigid motion of the whole beam. The resulting acceleratory force, however, is negligible for the small mass of the beam. Two physical mechanisms could be related to the tuning of the resonators properties. It was shown that for high acoustic powers SAW effectively modulate the internal damping mechanisms in the beam thus modifying its eigenfrequency [3,4]. On the other hand, the fast mechanical excitation of the resonator suspensions itself can result in a modulation of the resonator's dynamic properties. This can be demonstrated, for example, by an upside down pendulum [7]. A fast excitation (fast compared to the pendulum's resonance frequency) of the suspension shifts the equilibrium position even to the upside-down case, where the pendulum oscillates around the usually unstable zenith of the deflection. As the induced internal damping is related to the strain in the beam, whereas the 'fast excitation effect' is related to the ratio of the resonator amplitude to the acoustic excitation amplitude, these two effects should show contrary behavior when increasing the driving power at the beam. An increased, acoustically unloaded amplitude of the resonator results in larger strain within the beam. Hence, the eigenfrequency is expected to be modified by an

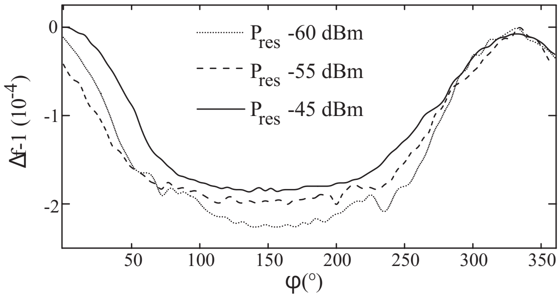

Fig. 4. Dependence of the relative frequency shift on phase between IDT_1 and ITD_2 for different driving powers at the beam. The magnitude of the observed shift decreases with increasing resonator driving power, being evidence for a non-dissipative tuning of the eigenfrequency.

increased amplitude via SAW-induced internal damping. If this shift is caused by the fast off-resonant excitation alone, it is expected to decrease as then the ratio of the beam amplitude to the excitation amplitude drops. In Fig. 4, we plot the dependence of the observed shift in eigenfrequency on the relative phase between IDT_1 and IDT_2, but this time for different applied driving powers at the beam. As the effect decreases with increasing excitation power at the beam, we conclude that the effect on the resonator's properties originate from the fast acoustic excitation of the beams suspensions.

We demonstrate the interaction between a nanomechanical resonator and a standing surface acoustic wave by shifting the wave nodes across the beam. The interaction is observed in terms of frequency shift and attenuation of the beam's resonant frequency. We probe the eigenfrequency and amplitude of the resonator by means of standard impedance spectroscopy, for which we used an equivalent circuit model. As the nanoresonator is sensitive to the acousto-mechanical excitation, its intrinsic properties like eigenfrequency and amplitude of motion directly reflect the pattern of the standing wave. We show that for relatively low acoustic power the modulation of the eigenfrequency is a consequence of the fast mechanical excitation of the beam's clamping points. At the highest acoustic powers the measured wave form deviates from a sine, which might be due to nonlinear effects mediated by the large SAW amplitudes to the resonator.

References

[1] X.M.H. Huang, C.A. Zorman, M. Mehregany, M.L. Roukes, Nature 421 (2003) 496.
[2] F.W. Beil, L. Pescini, E. Höhberger, A. Kraus, A. Erbe, R.H. Blick, Nanotechnology 14 (2003) 799.
[3] F.W. Beil, R.H. Blick, A. Wixforth, Proceedings of the IEEE Sensors 2002, Orlando, USA, 2002.
[4] F.W. Beil, R.H. Blick, A. Wixforth, Phys. Rev. Lett. (2003), submitted for publication.
[5] F.W. Beil, R.H. Blick, A. Wixforth, Physica E 13 (2002) 473.
[6] L.E. Kinsler, A.R. Frey, A.B. Coppers, J.V. Sanders, Fundamentals of Acoustics, Wiley, New York, 2000.
[7] D.J. Acheson, T. Mullin, Nature 366 (1993) 215.